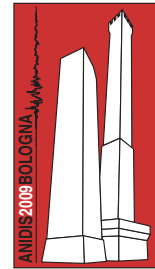


The combined MASW and ReMi methods for seismic geotechnical site characterization



Vitantonio Roma, PhD
Tecnimont
Corso Ferrucci 112/A, 10138 Torino
e-mail: v.roma@tecnimont.it; roma.vitantonio@libero.it

Rui Miguel Marques Moura, PhD
Geology Department University of Porto
Rua Campo Alegre 687 / 4169 - 007 Porto
e-mail: rmmoura@fc.up.pt

Keywords: MASW, REMI, geotechnical-seismic characterization, soil dynamics

ABSTRACT

For the seismic and dynamic design of the civil engineering projects a significant role is assumed by the geotechnical-seismic characterization of the site. The new Italian seismic code as well as the Eurocodes and other international seismic codes require the seismic site classification made on the basis of the shear wave velocity profile. Among the several techniques of site investigation the MASW method (Multichannel Analysis of Surface Waves) and the ReMi method (Refraction Microtremors) allow the determination of the shear wave velocity profile and hence the seismic site classification by means of the measurement and the consequent analysis of the Rayleigh waves. The article proposes a joint application of both the active MASW and the ReMi to a real case in order to compare the two complementary methods.

1 INTRODUCTION

The interest of both the scientific community and the professionals towards the MASW method (Multichannel Spectral Analysis of Surface Waves) has been increasing in the last years.

The reasons for such an interest are: 1) the increased consciousness that the design and the comprehension of the structures response to dynamic forces (earthquake, wind, vibrations, explosions, etc..) can be achieved only by identifying the dynamic properties and hence by determining the shear wave velocity profile V_s of the sites by means of a properly studied methodology; 2) the need of a relatively easy technique, which be sufficiently accurate and overcome some intrinsic drawbacks of other alternative techniques of investigation.

2 SEISMIC LOCAL EFFECTS AND SITE CLASSIFICATION

The local seismic classification of a site essentially consists of determining the category to which the site belongs on the basis of the main parameters which influence the site response to earthquakes or more generally to external dynamic forces. Currently there is an Italian code and several international codes, which classify the sites on the basis of their nature and their geotechnical characteristics, especially based on the vertical shear wave velocity profile V_s .

2.1 Italian and European Seismic Codes

The seismic classification provided by the new Italian seismic code O.P.C.M. n. 3274/2003 and also by the law D.M. 15/09/2005 "Ex Testo Unico sulle costruzioni" has been prepared following the same criteria adopted by the Eurocode 8. As a consequence there exists a satisfactory agreement between the site categories contemplated by the new Italian seismic code and the Eurocode 8 (see Table 1). With the

recent update D.M. 14/01/2008 some modifications have been applied to the criteria for classifying the sites of type A, B, C, D, E, S1, S2. Some new conditions have been introduced concerning the thickness of the soil overlaying the bedrock. These new conditions do not allow to consider some common sites, which in the authors' opinion should not be classified as special sites S2 as instead the referred laws does. As an example according to the new D.M. 14/01/2008 a site where the bedrock is at a depth of 25m should be classified as site S2, independently from its Vs30.

The same classification would be valid for a site with the Vs30 comprised between 360m/s and 800m/s and where the bedrock is at a depth of less than 30m. All these observations have already been evidenced in the journal *Ingegneria Sismica* n.3/2008.

2.2 The importance of Vs30

The new Italian seismic code OPCM 3274, as well as the Eurocode 8, if specific investigations are not available, determine the seismic design force on the basis of the seismic zone to which the site belongs. The Italian territory has been divided into 4 seismic zones, which are characterized by a peak ground acceleration a_g for the site of type A, that is surface rock or very stiff homogeneous soil (see table 1). When dealing with sites of type B, C, D, E, S1, S2 the seismic motion at the bedrock generally is different from the seismic motion at the free surface, depending on the intensity and the frequency content of the seismic input, on the thickness and the geotechnical characteristics of the soil overlaying the bedrock. If a specific analysis of wave propagation is not performed at the site, then the spectral seismic acceleration at the free surface can be evaluated by means of a factor S and a spectral shape provided by the seismic code. In the case of sites of type S1 and S2 the seismic code requires a specific analysis of the local seismic effects.

For the other types of site the classification is defined by means of the equivalent vertical shear wave velocity Vs30 within the first significant 30m of the site:

$$V_{s30} = \frac{30}{\sum_i^n \left(\frac{h_i}{V_{si}} \right)} \quad (1)$$

where V_{si} and h_i are the vertical shear wave velocity and the thickness of the i -th layer of the soil over the bedrock.

3 SEISMIC SITE CLASSIFICATION BY MEANS OF THE MASW METHOD

The MASW method is a non-invasive investigation technique (there is no need of boreholes), which allows to determine the vertical shear wave velocity V_s by measuring the propagation of the surface waves at several sensors (accelerometers or geophones) on the free surface of the site.

The main contribution to the surface waves is given by the Rayleigh waves, which travel through the upper part of the site at a speed, which is correlated to the stiffness of the ground.

In a layered soil Rayleigh waves are dispersive, that is Rayleigh waves with different wave length travel with a different speed (both phase and group velocities) (Achenbach, J.D., 1999, Aki, K. and Richards, P.G., 1980). Dispersion means that the apparent or effective phase (or group) velocity depends on the propagating frequency. This circumstance implies that high frequency waves with relatively short wave lengths contain information about the upper part of the site, instead low frequency waves with longer wave lengths provide information about the deeper layers of the site.

The MASW method can be applied as the active method or the passive method (Zywicki, D.J. 1999) or a combination of both active and passive. In the active method the surface waves are generated by a source located at a point on the free surface and then the wave motion is measured along a linear array of sensors. In the passive method the sensors can be located in arrays of different geometric shape: linear, circular, triangle, square, L shape, and the source is represented by the environmental noise, whose direction is not known a priori. The active method generally allows to determine an experimental apparent phase velocity (or dispersion curve) within the frequency range 5Hz -70Hz. Hence the active method can give information concerning the first 30m-35m, depending on the stiffness of the site. The passive method generally allows to define an experimental apparent phase velocity (or dispersion curve) within the frequency range 5Hz -15Hz. Hence the passive method can generally provide information about deeper layers, below 50m, depending on the stiffness of the site.

In the following both the active and the passive MASW methods will be explained and the combination of both will be applied to a real case. As passive method the ReMi procedure (Refraction Microtremors) will be used, since the results provided by the passive MASW and ReMi are equivalent.

The MASW method consists of three steps (Roma, 2002): (1) in the first step the experimental apparent phase velocity (or dispersion curve) is determined (**Figure 2**), (2) in the second step the numerical-theoretical apparent phase velocity (or dispersion

curve) is calculated (**Figure 5**), (3) in the last step the vertical shear wave velocity profile V_s is determined, by properly modifying the thickness h , the shear V_s and compressional V_p wave velocities (or in alternative to V_p it is possible to modify the Poisson's parameter ν), the mass density ρ of all the layers considered in the site model, until the optimal match between the experimental and the theoretical dispersion curves is achieved (**Figure 5**). During step 3 the site model and hence the shear wave velocity profile can be determined by means of a trial and error or an automatic procedures, or a combination of both. Usually the number of layers, the Poisson's parameter ν and the mass density ρ are assigned and successively the thickness and the shear wave velocity of the layers are modified. After the shear wave velocity profile has been determined, then the equivalent V_{s30} can be calculated and hence the seismic class of the site can be established (**Figure 6**).

It is meaningful to acquire any additional information about the geotechnical nature of the site, so that the existence of the special sites of type S1 and S2 can be recognized.

4 THEORETICAL BASIS OF THE MASW METHOD

The MASW method is based on the measurement and analysis of Rayleigh waves propagating through a layered half-space.

4.1 Dispersion and Attenuation of Rayleigh Waves

The existence of propagating of the Rayleigh waves into a layered half-space is searched by setting to zero the Rayleigh dispersion relation $R(f,k)$. The Rayleigh dispersion relation correlates the geometric and mechanical properties of the n layers of the layered half-space with the frequency f and the wave number k :

$$R(V_{s_i}, h_i, \nu_i, \rho_i, k, f) = 0, \quad i = 1/(n+1) \quad (2)$$

More details can be found in (Roma V. 2007, Roma V. 2001).

The search of the roots of the equation (2) can be performed by maintaining the frequency at a value f_0 and searching the wave numbers k which satisfy the equation (2). For a layered half-space the Dispersion relation (2) is multivalued, that is for a given value of frequency more than one wave number k may satisfy the relation (2). Each root of the equation (2), given by a couple of values (f, k) represents a simple wave or mode of Rayleigh, which can propagate through the

layered half-space. For a given frequency $\omega_0 = 2\pi f_0$, the first mode of Rayleigh, named the fundamental mode, corresponds to the greatest wave number, which satisfies equation (2). The other smaller wave numbers which satisfy equation (2) define the higher modes of Rayleigh. Hence equation (2) for a layered half-space establishes the existence of several modes of Rayleigh, which for an assigned frequency propagate at different phase and group velocities.

The physical interpretation of such a mathematical model is explained by the observation of the dispersion phenomenon, that is during the propagation of a wave train made of several simple Rayleigh waves, the several waves separate or disperse with increasing time and distance, since they travel at different velocities (**Figure 1**).

In addition to the dispersion phenomenon Rayleigh waves are subject to attenuation of their amplitude, caused by both geometric attenuation and dissipative attenuation. Geometric attenuation is due to the fact that the same energy is distributed to a cylindrical surface, which increases with distance from the source. The dissipative attenuation is caused by energy dissipation when particles oscillate around their equilibrium positions during the wave propagation (Roma V. 2003).

4.2 Apparent or Effective Dispersion Curve

The measurement of the surface waves along the sensors on the free surface of the ground gives the wave motion in the time-space domain (**Figure 1**). The perturbation generated by the point source contains all the several Rayleigh modes (S_v and P waves attenuates after few meters from the point source), which form a whole wave train and cannot be discerned nearby the point source. The dispersion of the Rayleigh modes can be completely observed only at an adequate distance from the point source (this distance is greater than about 100m in practice).

4.2.1 Experimental Dispersion Curve

When the wave field is transformed from the time-space domain into the frequency-wave number or equivalently into the frequency-phase velocity domain in order to show the dispersion relation equation (2), then it is observed that it is not possible to distinguish among the several Rayleigh modes as it is predicted by theory. Instead of the several Rayleigh modes, generally, only a unique apparent, also said effective, dispersion curve is observable (**Figure 2**). The experimental apparent dispersion curve obtained from the wave motion measured in field is the result of the

interaction among all the several modes of Rayleigh, also included the geometric array of sensors used for the measurement. In fact the geometric configuration of the sensors may influence the value of the apparent dispersion curve at certain frequencies (Roma V. 2001,b, Roma V. et al. 2002).

Depending on the geometric (thicknesses) and mechanical (V_s , V_p , ρ) of the ground layers, some modes of Rayleigh can appear as predominant with respect to the other modes at certain frequencies. Usually when the stiffness of the layers increases gradually with depth, then the first or fundamental mode of Rayleigh becomes predominant at every frequency.

Nevertheless several stratigraphies exist with stiff layers trapped between softer layers, or viceversa with soft layers trapped between stiffer layers, or more generally with a strong stiffness contrast between two consecutive layers, where higher modes of Rayleigh become predominant at certain frequencies. It may occur that at any frequencies there is not predominance of a unique mode, but two or more modes have the same energy. Under these conditions the apparent dispersion curve does not coincide with any mode of Rayleigh, since the apparent dispersion curve is the combination of all the predominant modes.

4.2.2 Theoretical-Numerical Dispersion Curve

The theoretical apparent or effective dispersion curve can be calculated once the modes of Rayleigh have been determined (Figura 4). To reach this purpose several methods exist, such as the Roma's method and the Lai and Rix method (Roma V. 2001,b, Roma V. 2007,b).

It can be demonstrated that the theoretical apparent dispersion curve determined by the Roma's procedure coincides with the theoretical effective dispersion curve determined by Lai and Rix procedure, if proper conditions about the smoothness of the dispersion curve are respected (Roma V. 2000, Roma V. 2007,b).

The theoretical apparent dispersion curve determined by Roma's procedure is calculated in the same manner followed in determining the experimental dispersion curve. The only diversity concerns the way in which the spectrum (f-k) of the wave field is obtained. The experimental (f-k) spectrum is obtained by a 2D Fourier transform of the time-space wave field, instead the numerical (f-k) spectrum is obtained by only 1D Fourier transform, applied to the Green's function of the layered halfspace.

Alternatively the numerical apparent dispersion curve can be determined by using the Lai and Rix procedure (Lai, 1998), which is based on the physical

concept that wave train of all the modes of Rayleigh can be considered as a unique complex perturbation, where all the modes of Rayleigh form a unique wave phase.

5 THE REMI METHOD

The ReMi (Refraction Microtremors) method has been developed by Louie (Louie, 2001). It consists of three steps, the same as the MASW method: the first step concerns the determination of the experimental dispersion curve of Rayleigh waves; the second step coincides with the calculation of the numerical apparent dispersion curve and the third step consists of inverting the apparent dispersion curve in order to find the vertical shear wave profile of the site. In the ReMi method the experimental dispersion curve is obtained passing from the (t-x) domain gathered on site to the (p-f) domain by means of a p-tau transformation, or slantstack and a successive Fourier transform. Following the indications given by Louie (Louie, 2001) the p-tau transformation can be written as:

$$A(p, \tau) = \int_x A(x, t = \tau + px) dx \quad (3)$$

where the slope of the line $p = dt/dx$ is the inverse of the apparent velocity V_a in the x direction.

The next step takes each p-tau trace in $A(p, \tau)$ equation (3) and computes its complex Fourier transform in the tau or intercept time direction:

$$F_A(p, f) = \int_{\tau} A(p, \tau) e^{-i2\pi f \cdot \tau} d\tau \quad (4)$$

The power spectrum $S(p, f)$ is the magnitude squared of the complex Fourier transform:

$$S_A(p, f) = F_A^*(p, f) \cdot F_A(p, f) \quad (5)$$

where the * denotes the complex conjugate.

This completes the transform of a record from distance-time (x-t) into p-frequency (p-f) space.

The ray parameter p for these records is the horizontal component of slowness (inverse velocity) along the array. This means that once the spectrum and the experimental dispersion curve in the (p-f) domain have been evaluated, then it is straightforward to calculate the experimental dispersion curve in the (v-f) domain.

5.1 Picking the Experimental Dispersion Curve

In his article Louie explains that the experimental dispersion curve should be obtained from the spectrum in the (p-f) domain by picking not the maxima of the spectrum, but the lower edge of the lowest-velocity, but still reasonable peak ratio. He says that the reason for such a procedure is that the arrays are linear and do not record an on-line triggered source, so some noise energy will arrive obliquely and appear on the slowness-frequency images as peaks at apparent velocities V_a higher than the real in-line phase velocity v :

$$V_a = v/\cos(a) = 1/p \quad (6)$$

Where

$$a = \cos^{-1}(vp) \quad (7)$$

with “a” being the propagation angle off the line direction.

Louie also mentions that picking the lower bound of the spectrum will exclude noise and higher modes of Rayleigh, hence only the fundamental mode of Rayleigh will form the experimental dispersion curve. It is also said that if it is known that the source direction aligned with the array (i.e. $a=0$), then the maxima of the spectrum must be picked instead of the lower bound.

In the authors’ opinion Louie’s considerations about the direction a of the source are valid only if the spectrum in the (p-f) domain is calculated using the horizontal component of the Rayleigh wave field. Since the Rayleigh waves form an ellipse shaped wave motion during propagation, the wave motion can be decomposed into the vertical and the horizontal components. The direction of the source “a” influences the intensity of the horizontal component projected along the array direction, but not the vertical component.

Hence if only the vertical component of the wave field is measured and successively analyzed to calculate the spectrum, then the direction of the source “a” does not influence the spectrum itself.

This implies that the picking for the apparent experimental dispersion curve should be done taking the maxima of the spectrum, in the same way it is done in the MASW procedure.

This consideration can be proved to be valid in the example shown in the following. We have overlapped the experimental dispersion curve obtained with the active MASW method with the spectrum in the (p-f) domain provided by the ReMi method. As it can be observed (**Figure 4**) the peaks of the MASW (f-k) spectrum coincide better with the maxima of the

REMI (v-f) spectrum rather than the lower edge of the spectrum.

6 APPLICATION OF BOTH MASW AND REMI TO A REAL CASE

The active MASW method allows to obtain information within the frequency range 10Hz-100Hz, hence it provides information within the first 30m of the site. Instead the ReMi (Refraction Microtremors) method allows to obtain information within the frequency range 1Hz-15Hz, depending on the available environmental noise, hence it can give information about layers deeper than 30m, potentially down to 100m, as it is stated by Louie (2001). In this regard the ReMi method is equivalent to the passive MASW. By combining the information gained with the active MASW and the ReMi methods it is possible to cover the whole frequency range of interest in the seismic site characterization 1Hz-100Hz, reaching depths greater than the 30m which are required by the international codes to evaluate the V_{s30} . The site is located near the Eurocentre of Pavia. Both the active MASW and the ReMi tests have been performed.

The parameters of the active MASW tests are:

- Geophones interspace = 1m
- Source type = hammer
- Delta time of acquisition = 0.5ms
- Source location = 2m from first geophone
- Total time of acquisition = 4 s
- Number of geophones = 24

The data has been processed by means of the software MASW (www.masw.it).

In **Figure 1** it is shown the time-space vertical wave motion, instead in **Figure 2** the (f-k) spectrum and the experimental dispersion curve are illustrated.

For the same site the parameters of the ReMi test are:

- Geophones interspace = 1m
- Source type = environmental noise
- Delta time of acquisition = 2ms
- Total time of acquisition = 32s
- Number of geophones = 24

In **Figure 3** the environmental noise is reported, measured during 32s of acquisition.

In **Figure 4** the (f-v) spectrum obtained with ReMi method is shown, together with the experimental dispersion curve calculated with the active MASW method. In this case the total length of

the geophones array used for the ReMi test is limited to 24m, so the minimum frequency containing useful information is 5Hz. Anyway it can be observed that there is very good agreement between the MASW and ReMi methods, if the maxima of the spectrum are considered in ReMi procedure, instead of the lower edge of the spectrum as suggested by Louie (2001).

In **Figure 5** is illustrated the comparison between the experimental and the numerical dispersion curves, with a relative error of 12%. In **Figure 5** the final Vs profile is shown, with the shadow zone which represents the associated error of the most probable Vs profile.

According to this Vs profile the Vs30 is equal to 490m/s and following the Eurocode 8 and the OPCM 3274 the site is classified as type B (**Figure 6**).

REFERENCES (STYLE REFERENCE TITLE)

- Bergamaschi M., Locatelli L., Quadrelli D., Roma V. "Soil-Structure dynamic interaction: application to design and construction of the facilities of a gas power plant", XIIIth Danube-European Conference on Geotechnical Engineering (29-31 May 2006, Lubiana) Active Geotechnical Design in Infrastructure Development
- D.M. 16.01.1996: "Norme tecniche per le costruzioni in zone sismiche".
- D.M. 14/09/2005: "Norme tecniche per le costruzioni"
- D.M. 14/01/2008: "Norme tecniche per le costruzioni"
- Circolare 2/02/2009 contenente le Istruzioni per l'applicazione delle "Nuove norme tecniche per le costruzioni" di cui al D.M. 14/09/2008.
- De Stefano A., Foti S., Lancellotta R., Roma V.: "L'isolamento sismico delle strutture su pali", Atti del IX Convegno Nazionale di Ingegneria Sismica in Italia, Torino 20-23 Settembre 1999
- De Stefano A., Foti S., Lancellotta R., Roma V.: "Dissipazione dell'energia in strutture su pali", Atti del IX Convegno Nazionale di Ingegneria Sismica in Italia, Torino 20-23 Settembre 1999
- Foti S., Lai C.G., Rix G., Roma V.: "Simultaneous measurement and inversion of surface wave dispersion and attenuation curves", Soil Dynamics and Earthquake Engineering 22 (2002) 923-930
- Hebeler G., Lai C.G., Orozco C., Rix G., Roma V.: "Recent advances in Surface Wave methods for Geotechnical Site Characterization", XV International Conference on Soil Mechanics and Geotechnical Engineering, Istanbul 27-31 Agosto 2001
- Louie J.N.: "Faster, Better: Shear-Wave Velocity to 100 Meters Depth from Refraction Microtremor Arrays", *Bulletin of the Seismological Society of America*; April 2001; v. 91; no. 2; p. 347-364;
- Mahtab A., Stanton K.L., Roma V. "Environmental Impacts of Blasting for Stone Quarries near Bay of Fundy", 6th Bay of Fundy Workshop, September 29-October 2, 2004, Cornwallis Park, Nova Scotia.
- OPCM n. 3274 del 20/03/03 del Consiglio dei ministri – Allegato 1 – "Criteri per l'individuazione delle zone sismiche – Individuazione, formazione e aggiornamento degli elenchi nelle medesime zone".

- OPCM n. 3274 del 20/03/03 del Consiglio dei ministri – Allegato 4 – "Norme Tecniche per il progetto sismico delle opere di fondazione e sostegno dei terreni".
- OPCM n.3316 - Modifiche ed integrazioni all'Ordinanza del Presidente del Consiglio dei Ministri n.3274 del 20.03.03.
- Roma V., Lancellotta R., Rix G.: "–Frequencies and wavenumbers of Resonance in horizontally stratified media for traveling Rayleigh waves ", XI International Conference on Waves and Stability in Continuous Media, Porto Ercole 3-9 Giugno 2001
- Roma V., Hebeler G., Rix G., Lai C.G.: " Geotechnical soil characterization using fundamental and higher Rayleigh modes propagation in layered media ", XII European Conference on Earthquake Engineering, London 9-13 Settembre 2002
- Roma V.: "Automated inversion of Rayleigh geometrical dispersion relation for geotechnical soil identification ", 3rd World Conference on Structural Control, Como 7-12 April 2002
- Roma V.: "Soil Properties and Site characterization through Rayleigh Waves", International Conference on Pre-failure Deformation Characteristics of Geomaterials, Lione, Settembre 2003
- Roma V.: "Dynamic Soil Identification by means of Rayleigh Waves", XI Conferenza Nazionale di Ingegneria Sismica in Italia, Genova, Gennaio 2004
- Roma, V. and Mahtab, M. A. "Use of Rayleigh Waves as Reference for Determining Setback Distances for Explosions near Shorelines", Poster Session, 6th Bay of Fundy Workshop, September 29-October 2, 2004, Cornwallis Park, Nova Scotia.
- Roma V., Pescatore M.: "Environmental impact caused by high speed train vibrations", International Geotechnical Conference: Soil-structure interaction: calculation methods and engineering practice, 26-28 May, 2005, St. Petersburg (accettato per pubblicazione)
- Roma V.: "Impatto ambientale causato da vibrazioni prodotte da treni ad alta velocità ", XII Conferenza Nazionale di Ingegneria Sismica in Italia, Pisa, Giugno 2007
- Roma V.: "Caratterizzazione geotecnica sismica dei suoli con il metodo MASW", XII Conferenza Nazionale di Ingegneria Sismica in Italia, Pisa, Giugno 2007
- Roma V. "Caratterizzazione geotecnica sismica dei suoli con il metodo MASW", testo e manuale del software MASW, sul sito www.masw.it

Table 1. Seismic site classification according to O.P.C.M. n. 3274/2003, D.M. 15/09/2005 and Eurocode 8.

Ground type	Description of stratigraphic profile	Parameters		
		$v_{s,30}$ (m/s)	N_{SPT} (blows/30cm)	c_u (kPa)
A	Rock or other rock-like geological formation, including at most 5 m of weaker material at the surface	> 800	–	–
B	Deposits of very dense sand, gravel, or very stiff clay, at least several tens of m in thickness, characterised by a gradual increase of mechanical properties with depth	360 – 800	> 50	> 250
C	Deep deposits of dense or medium-dense sand, gravel or stiff clay with thickness from several tens to many hundreds of m	180 – 360	15 - 50	70 - 250
D	Deposits of loose-to-medium cohesionless soil (with or without some soft cohesive layers), or of predominantly soft-to-firm cohesive soil	< 180	< 15	< 70
E	A soil profile consisting of a surface alluvium layer with v_s values of type C or D and thickness varying between about 5 m and 20 m, underlain by stiffer material with $v_s > 800$ m/s			
S_1	Deposits consisting – or containing a layer at least 10 m thick – of soft clays/silts with high plasticity index (PI > 40) and high water content	< 100 (indicative)	–	10 - 20
S_2	Deposits of liquefiable soils, of sensitive clays, or any other soil profile not included in types A – E or S_1			

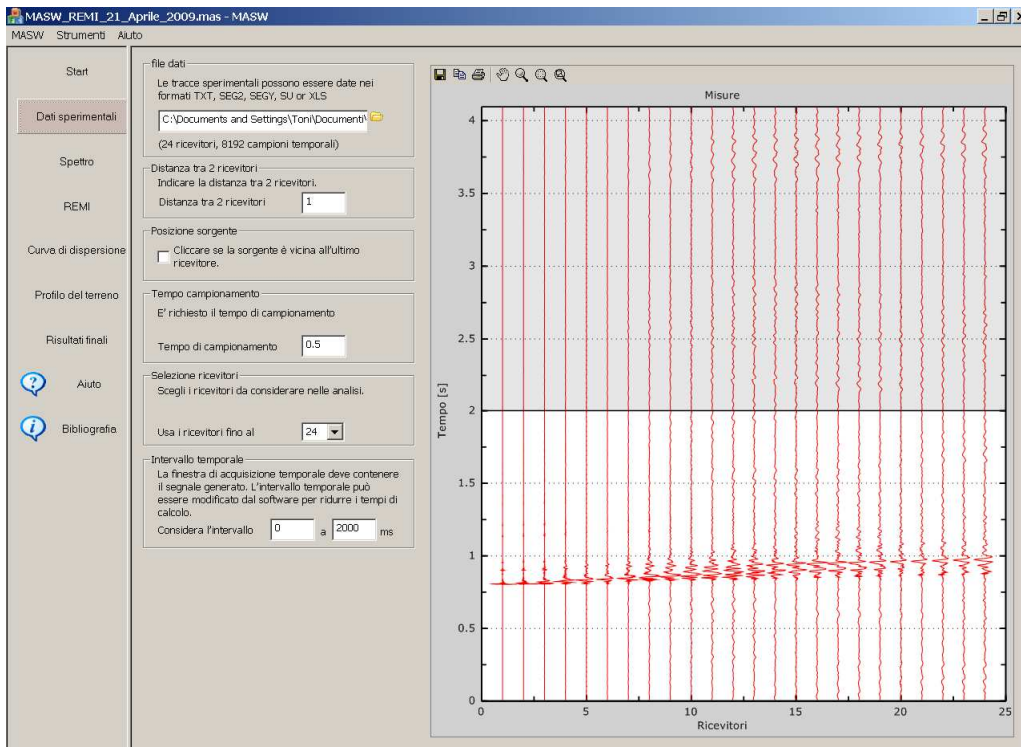


Figure 1: vertical wave motion (hammer source) for the active MASW.

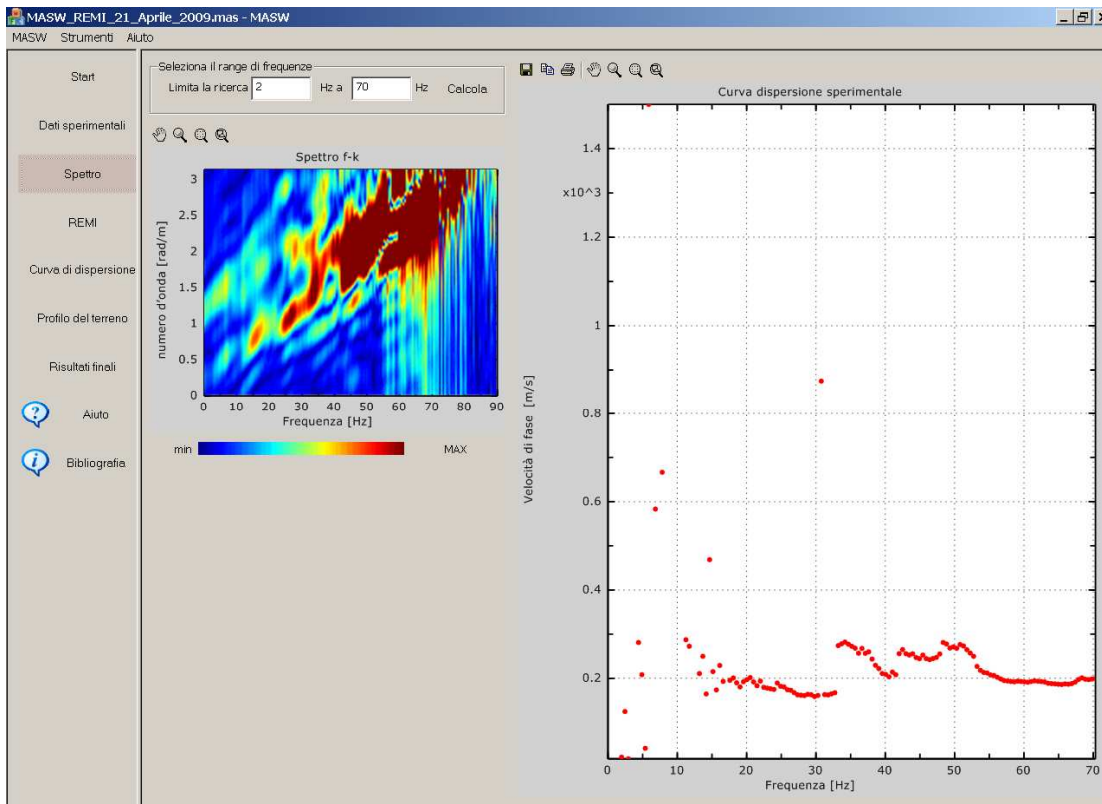


Figure 2: (f-k) spectrum and experimental dispersion curve with active MASW.

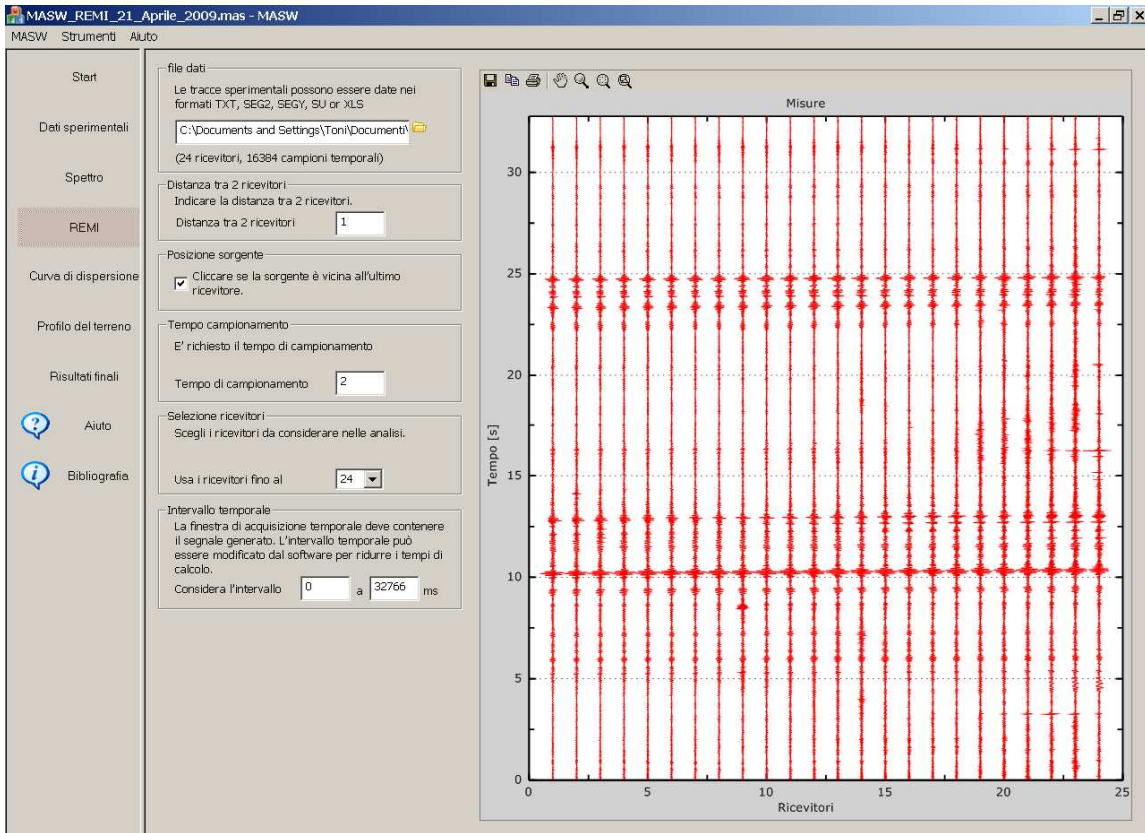


Figure 3: vertical wave motion (environmental noise) for the ReMi.

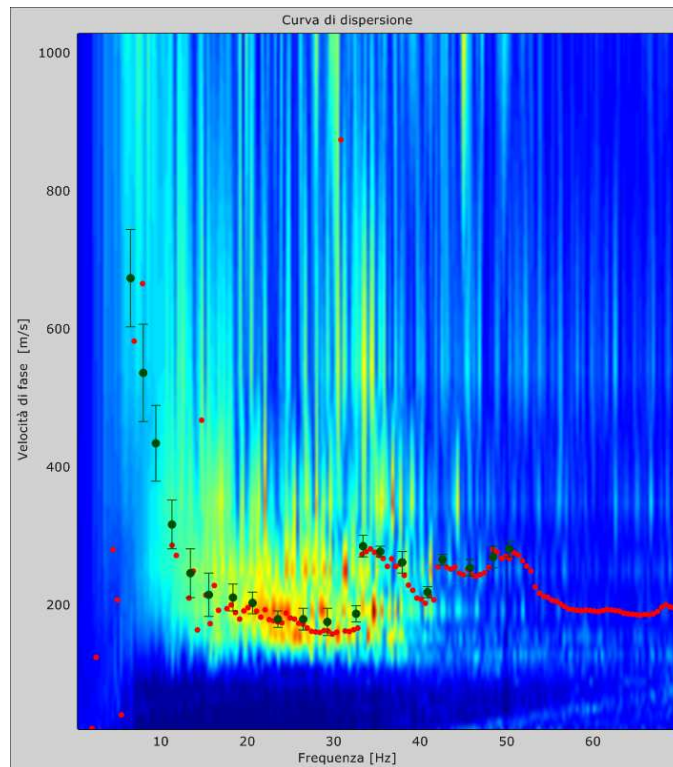


Figure 4: ReMi spectrum together with the active MASW experimental dispersion curve.

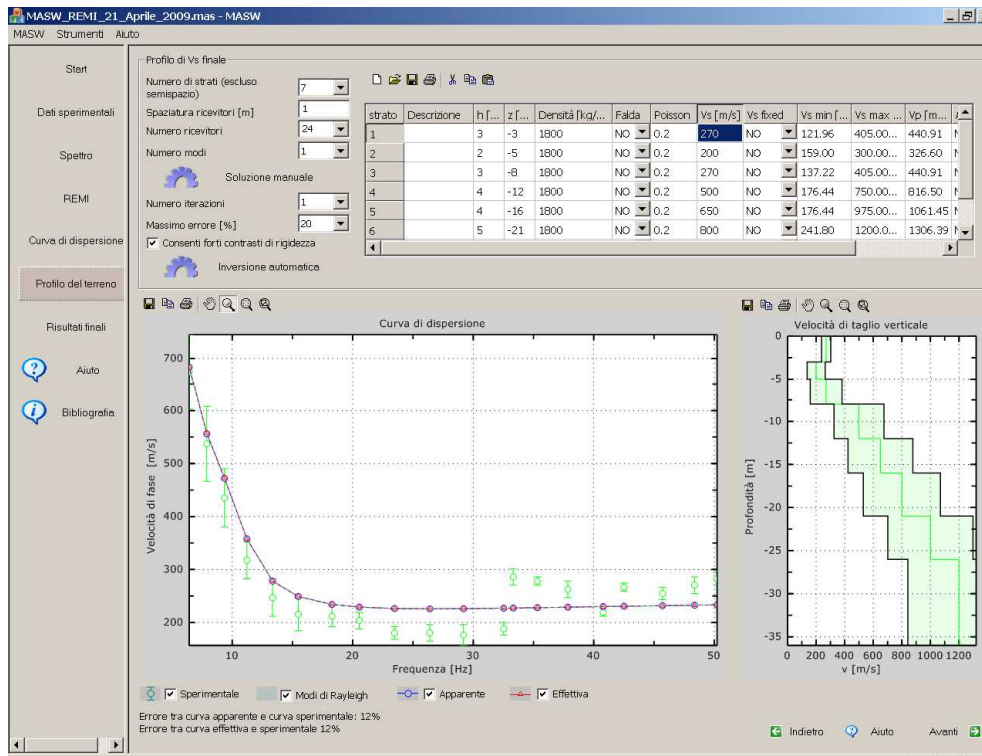


Figure 5: Numerical and Experimental dispersion curves (left side) and final shear wave velocity profile Vs.

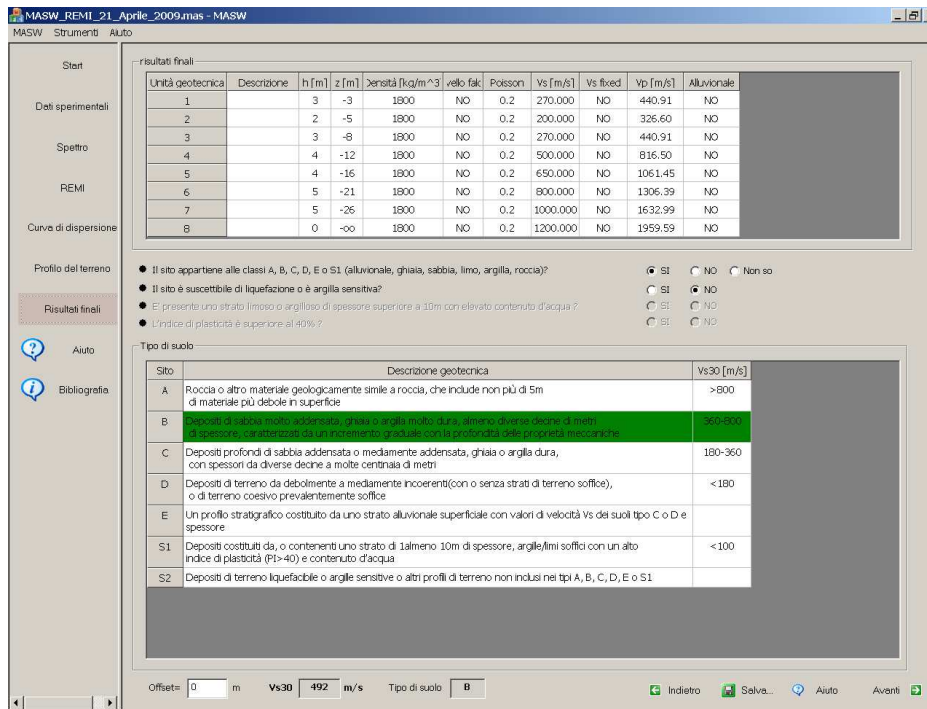


Figure 6: Site seismic classification based on Vs30.